Published in final edited form as:
J Cell Physiol. 2010 November ; 225(3): 855–864. doi:10.1002/jcp.22296.

Agents That Bind Annexin A2 Suppress Ocular Neovascularization

RAQUEL LIMA E SILVA[1], **JIKUI SHEN**[1], **YUAN YUAN GONG**[1], **CHRISTOPHER P. SEIDEL**[1], **SEAN F. HACKETT**[1], **KAMALA KESAVAN**[2], **DOUGLAS B. JACOBY**[2], and **PETER A. CAMPOCHIARO**[1,†,*]

[1]Department of Ophthalmology and Neuroscience, The Johns Hopkins University School of Medicine, Baltimore, Maryland [2]TransMolecular, Inc., King of Prussia, Pennsylvania

Abstract

TM601 is a synthetic polypeptide with sequence derived from the venom of the scorpion *Leiurus quinquestriatus* that has anti-neoplastic activity. It has recently been demonstrated to bind annexin A2 on cultured tumor and vascular endothelial cells and to suppress blood vessel growth on chick chorioallantoic membrane. In this study, we investigated the effects of TM601 in models of ocular neovascularization (NV). When administered by intraocular injection, intravenous injections, or periocular injections, TM601 significantly suppressed the development of choroidal NV at rupture sites in Bruch's membrane. Treatment of established choroidal NV with TM601 caused apoptosis of endothelial cells and regression of the NV. TM601 suppressed ischemia-induced and vascular endothelial growth factor-induced retinal NV and reduced excess vascular permeability induced by vascular endothelial growth factor. Immunostaining with an antibody directed against TM601 showed that after intraocular or periocular injection, TM601 selectively bound to choroidal or retinal NV and co-localized with annexin A2, which is undetectable in normal retinal and choroidal vessels, but is upregulated in endothelial cells participating in choroidal or retinal NV. Intraocular injection of plasminogen or tissue plasminogen activator, which like TM601 bind to annexin A2, also suppressed retinal NV. This study supports the hypothesis that annexin A2 is an important target for treatment of neovascular diseases and suggests that TM601, through its interaction with annexin A2, causes suppression and regression of ocular NV and reduces vascular leakage and thus may provide a new treatment for blinding diseases such as neovascular age-related macular degeneration and diabetic retinopathy.

Chlorotoxin is a 36-amino-acid, 3.95 kDa peptide isolated from the venom of the scorpion *Leiurus quinquestriatus* (DeBin et al., 1993). It acts to immobilize insects and other invertebrates that are bitten by transiently blocking chloride channels and disrupting neuronal transmission. While studying its effects on chloride channels in cultured cells, it was noted that chlorotoxin differentially binds to malignant cells (Soroceanu et al., 1998;

---

*Correspondence to: Peter A. Campochiaro, Maumenee 719, The Johns Hopkins University School of Medicine, 600 N. Wolfe Street, Baltimore, MD 21287-9277. pcampo@jhmi.edu.
†George S. and Dolores Dore Eccles Professor of Ophthalmology and Neuroscience.
Raquel Lima e Silva and Jikui Shen contributed equally to this work.

Ullrich et al., 1998). TM601 is a synthetically produced chlorotoxin that was found to be safe and well-tolerated when injected into animals. When labeled with ^{131}I, TM601 directs radiation to gliomas allowing imaging of tumor cells and providing anti-tumor effects (Hockaday et al., 2005; Shen et al., 2005). In a phase I study, in which 17 patients with glioblastoma multiforme and 1 with anaplastic astrocytoma had ^{131}I-TM601 injected into the tumor cavity, the ^{131}I-TM601 bound to the wall of the cavity and was visualized for several days (Mamelak et al., 2006). Seven of 16 patients for whom radiographic follow-up was available at 90 days were felt to be stable and nine showed evidence of progression. This small study confirmed that TM601 differentially binds to tumor tissue and could be used to target radiation treatment to tumors.

The mechanism of the anti-neoplastic effect of TM601 is not completely understood, but a recent study has suggested that suppression of tumor angiogenesis might contribute, because TM601 suppresses angiogenesis surrounding tumor cells implanted on chick chorioallantoic membranes (Jacoby et al., 2010). TM601 binds to annexin A2 on the surface of cells from several tumor cell lines and human umbilical vein endothelial cells (Kesavan et al., 2010) and annexin A2 has been implicated in angiogenesis. Recent studies have demonstrated that the expression of annexin A2 is increased in several types of tumor cells (Sharma and Sharma, 2007).

Agents that have antiangiogenic activity in one setting do not necessarily exert antiangiogenic activity in other vascular beds (Campochiaro, 2006). Ocular neovascularization provides an important area to test agents with potential antiangiogenic activity, because there are well-established models for diseases that are prevalent and clinically important. Choroidal neovascularization, which occurs in patients with age-related macular degeneration (AMD) the most common cause of severe vision loss in elderly Americans (Klein et al., 1992), is modeled in mice with laser-induced rupture of Bruch's membrane (Tobe et al., 1998b) and transgenic mice in which the *rhodopsin* promoter drives expression of vascular endothelial growth factor (VEGF) in photoreceptors (rho/VEGF mice) (Okamoto et al., 1997). It should be noted that these models do not recapitulate all of the features of neovascular AMD, but both have shown predictive value for results seen in clinical trials for neovascular AMD (Saishin et al., 2003; Nguyen et al., 2006a, 2009a). Retinal neovascularization, which occurs in diabetic retinopathy, the most common cause of severe vision loss in working-aged Americans (Klein et al., 1984), is modeled by oxygen-induced ischemic retinopathy (Smith et al., 1994). This model is most analogous to retinopathy of prematurity, but like proliferative diabetic retinopathy, the critical feature is that VEGF is produced by ischemic retina and causes retinal NV. In this study, we investigated the effects of TM601 and annexin A2 in these models of ocular neovascularization.

Materials and Methods

Mouse model of laser-induced choroidal NV

Mice were treated in accordance with the Association for Research in Vision and Ophthalmology guidelines for the use of animals in research. Choroidal NV was induced by laser photocoagulation-induced rupture of Bruch's membrane as previously described (Tobe

et al., 1998b). Briefly, 5- to 6-week-old female C57BL/6 mice were anesthetized and pupils were dilated with 1% tropicamide. Three burns of 532 nm diode laser photocoagulation (75 μm spot size, 0.1 sec duration, 120 mW) were delivered to each retina with the slit lamp delivery system of an OcuLight GL diode laser (Iridex, Mountain View, CA) using a handheld cover slip as a contact lens to view the retina. Burns were performed in the 9, 12, and 3 o'clock positions of the posterior pole of the retina. Production of a bubble at the time of laser, which indicates rupture of Bruch's membrane, is an important factor in obtaining choroidal NV, and therefore, only burns in which a bubble was produced were included in the study.

Treatments were begun immediately after rupture of Bruch's membrane and included (1) intravitreous injection of 1 μl of vehicle or vehicle containing 150 μg of TM601 immediately after laser treatment, (2) daily periocular injections of 5 μl of vehicle or vehicle containing 10, 50, 250, or 1,000 μg, or (3) intravenous injections of vehicle or 20 mg/ml of TM601 three times a week. Fourteen days after laser, the area of choroidal NV at Bruch's membrane rupture sites was measured.

To assess the effect of TM601 on established choroidal NV, mice had rupture of Bruch's membrane at three locations in each eye and after 7 days a cohort of mice had measurement of the baseline area of NV at Bruch's membrane rupture sites. The remaining mice were treated with TM601 or vehicle between 7 and 14 days followed by measurement of the area of choroidal NV at Bruch's membrane rupture sites.

Measurement of the area of choroidal NV at Bruch's membrane ruptures sites

Two weeks after rupture of Bruch's membrane, mice were perfused with 1 ml of phosphate-buffered saline (PBS) containing 50 mg/ml of fluorescein-labeled dextran (2×10^6 average molecular weight, Sigma–Aldrich, St. Louis, MO) and choroidal flat mounts were prepared as previously described (Mori et al., 2001). Briefly, the eyes were removed, fixed for 1 h in 10% phosphate-buffered formalin, and the cornea and lens were removed. The entire retina was carefully dissected from the eyecup, radial cuts were made from the edge of the eyecup to the equator in all four quadrants, and it was flat-mounted in aqueous mounting medium (Aquamount; Polysciences, Warrington, PA). Flat-mounts were examined by fluorescence microscopy (Axioskop; Carl Zeiss Meditec, Thornwood, NY), and images were digitized with a three charge-coupled device color video camera (IK-TU40A; Toshiba, Tokyo, Japan) and a frame grabber. Image-analysis software (Image-Pro Plus; Media Cybernetics, Silver Spring, MD) was used to measure the area of each choroidal NV lesion with the investigator masked with respect to treatment group.

Mice with oxygen-induced ischemic retinopathy

Ischemic retinopathy was produced in neonatal C57BL/6 mice as previously described (Lima e Silva et al., 2007; Xie et al., 2008). At postnatal day 7 (P7), litters of C57BL/6 mice were placed in an airtight incubator and exposed to an atmosphere of 75 ± 3% oxygen for 5 days. They were returned to room air at P12 and given an intraocular injection of 1 μl of vehicle or vehicle containing 50 μg of TM601. The area of NV on the surface of the retina was measured as previously described (Shen et al., 2007; Xie et al., 2008). Briefly, P17 mice

were given an intraocular injection of 1 μl of rat anti-mouse platelet endothelial cell adhesion molecule-1 (PECAM-1) antibody (Pharmingen, San Jose, CA) under a dissecting microscope with a Harvard Pump Microinjection System and pulled glass micropipettes. Mice were euthanized 12 h after injection and eyes were fixed in phosphate-buffered formalin for 5 h at room temperature. Retinas were dissected, washed, and incubated with goat-anti-rat polyclonal antibody conjugated with Alexa Fluor 488 1:500 (Invitrogen, Carlsbad, CA) at room temperature for 45 min and then flat mounted. An observer masked with respect to treatment group measured the area of NV per retina by image analysis.

Transgenic mice with vascular endothelial growth factor (VEGF)-induced NV

Transgenic mice in which the *rhodopsin* promoter drives expression of VEGF in photoreceptors have the onset of VEGF production in photoreceptors at P7 and develop extensive NV along the outer surface of the retina by P21 (Okamoto et al., 1997; Tobe et al., 1998a). Mice hemizygous for the transgene were given daily periocular injections of 3 μl of vehicle or vehicle containing 150 μg of TM601 between P7 and P21 and then euthanized and the amount of subretinal NV was measured. Mice were anesthetized, perfused with fluorescein-labeled dextran, and the total area of neovascularization on the outer surface of the retina was measured on retinal flat mounts by image analysis (Tobe et al., 1998a).

Terminal deoxynucleotidyl transferase (TdT)-mediated dUTP nick end labeling (TUNEL)

Seven days after laser-induced rupture of Bruch's membrane, adult female C57BL/6 mice received daily periocular injections of 5 μl of vehicle or vehicle containing 50 μg of TM601 or a single intravitreous injection of 1 μl of vehicle or vehicle containing 50 μg of TM601 and after 2 days the mice were euthanized, eyes were frozen in optimal cutting temperature compound and 10 μm serial sections were cut through areas of choroidal NV. Slides were immersed in 1% paraformaldehyde for 10 min at room temperature and TUNEL was performed with an ApopTag kit (ApopTag Fluorescein Red; Intergen, Purchase, NY) according to the manufacture's instructions. After TUNEL, some slides were incubated at 25°C for 1 h with 1:100 *Griffonia simplicifolia* lectin B4 fluorescein isothiocyanate (Vector Laboratories, Burlingame, CA). Stained flat mounts and sections were examined with a fluorescence microscope (Nikon Instruments, Inc., New York, NY) using SPOT RT 3.4 software.

Immunofluorescent staining

Seven days after laser-induced rupture of Bruch's membrane, adult female C57BL/6 mice received a single intraocular injection of PBS or 50 μg of TM601 or daily periocular injections of 50 μg of TM601 or PBS. After 9 days, mice were euthanized and eyes were removed for immunohistochemical staining. At P12, mice with ischemic retinopathy were given an intraocular injection of 50 μg of TM601 and at P16 the mice were euthanized and eyes were removed. Some eyes were frozen and 10 μm frozen ocular sections were stored at −80°C. Other eyes were used for staining of whole retina or choroid. They were fixed in 10% phosphate-buffered formalin for 4 h and then retinas were removed. Retinas or eyecups were blocked with 8% normal goat serum and then incubated with one or a mixture of rabbit anti-TM601 (1:500, TransMolecular, Inc., King of Prussia, PA), mouse monoclonal anti-

annexin A2 (1:100, BD Biosciences, San Jose, CA), or rat anti-mouse PECAM1 at room temperature for 2 h. After three washes, eyecups were incubated for 45 min at room temperature with secondary antibody, either Alexa Fluor 594-labeled goat anti-rabbit immunoglobulin (IgG), Alexa Fluor 488-labeled goat anti-rat IgG, or Alexa Fluor 488-labeled goat ant-mouse IgG. Retinal and choroidal flat mounts were prepared. Frozen sections were dried and fixed with 4% paraformaldehyde, blocked with 8% normal donkey serum, and incubated overnight in rabbit anti-TM601 (1:500) and mouse anti-annexin A2 (1:100). After three washes, eyecups were incubated for 45 min at 25°C with secondary antibody, either Alexa Fluor 594-labeled goat anti-rabbit IgG or Alexa 488-labeled goat anti-mouse IgG. Stained flat mounts and sections were examined by fluorescence microscopy.

Retinal vascular permeability

Four- to five-week-old C57BL/6 mice were given an intraocular injection of 200 ng of VEGF, a mixture of 200 ng of VEGF and 50 μg of TM601, or vehicle and euthanized after 6 h. Eyes were removed and fixed in 10% formalin for 4 h. Retinas were dissected, washed three times, and incubated in 8% normal donkey serum for 40 min at room temperature. Retinas were incubated overnight in rabbit anti-mouse albumin antibody in 0.1% Triton, washed three times in PBS containing 0.1% Triton, and incubated in Cy3-conjugated donkey anti-rabbit IgG (Jackson ImmunoResearch Laboratories, Inc., West Grove, PA) for 50 min at room temperature. After washing, retinal whole mounts were prepared and examined by fluorescence microscopy using an Axioskop microscope (Carl Zeiss Meditec). The area of albumin staining per retina was measured by image analysis with the investigator masked with respect to treatment group.

Statistical analyses

Statistical comparisons for treatment effects in each experiment were done with linear regression models using generalized estimating equations population-averaged models and mixed-effects model regression. For the laser-induced choroidal NV model, the analysis included up to three choroidal NV area measurements per eye. All measurements from either eye of a mouse were assumed to be exchangeable when modeling correlation structure and were assumed to be subject to nonerror variability, due only to treatment for experiments in which different treatments were administered to each eye of the mouse. An overall test for treatment effect was first performed in all models, and if the overall test indicated a significant treatment effect, individual treatments were compared with the vehicle treatment by using linear contrasts. The Bonferroni or Dunnett procedure was used to adjust for multiple comparisons. When necessary, a log transformation of measurements before analysis was used so that the distribution of measurements better met the normally distributed outcome assumption of the linear mixed model. All analyses were performed on computer (SAS software; SAS Institute, Inc., Cary, NC).

Results

TM601 given by several different routes of administration suppresses choroidal NV

Adult C57BL/6 mice were given an intraocular injection of vehicle or vehicle containing 50 μg of TM601 at the time of rupture of Bruch's membrane with laser photocoagulation. After 2 weeks, the mice were perfused with fluorescein-labeled dextran and choroidal flat mounts were examined by fluorescence microscopy. The area of choroidal NV at Bruch's membrane rupture sites was significantly smaller in eyes that had been injected with TM601 (Fig. 1A,C) compared to those that had been injected with vehicle (Fig. 1B,C). Intravenous injection of 20 mg/kg of TM601 three times a week also significantly reduced the development of choroidal NV (Fig. 1D–F). A range of doses of TM601 was given by daily periocular injection for 2 weeks after rupture of Bruch's membrane and even the lowest dose of 10 μg resulted in small choroidal NV lesions (Fig. 1G) and the mean area of NV was significantly less than that in eyes of a separate control group of mice treated with daily periocular injections of vehicle (Fig. 1J). Doses of 50 μg (Fig. 1H) or higher caused significant suppression of choroidal NV (Fig. 1J) due primarily to local penetration of TM601 through the sclera and not absorption into the systemic circulation, because eyes treated with 50 μg or higher had significantly less NV than untreated fellow eyes. Eyes injected with 10 μg did not have significantly less NV than their fellow eyes, but this is likely to be because this dose is near the lower limit of effective doses rather than an indication of a systemic effect.

Administration of TM601 after choroidal NV is established causes regression of the NV due to apoptosis of endothelial cells

Bruch's membrane was ruptured by laser photocoagulation in several mice and after 7 days a cohort of the mice were perfused with fluorescein-labeled dextran and the baseline area of choroidal NV was measured. The remainder of the mice received an intraocular injection of 50 μg of TM601 in one eye or vehicle in the fellow eye and after 1 week the area of choroidal NV at Bruch's membrane rupture sites was measured. Eyes injected with TM601 at 1 week showed significantly less choroidal NV (Fig. 2A,D) at 2 weeks than eyes injected with vehicle (Fig. 2B,D). They also had less choroidal NV than the baseline amount that was present at 1 week (Fig. 2C,D). This indicates that TM601 caused regression of choroidal NV.

Mice had rupture of Bruch's membrane and after 1 week had an intraocular injection of 50 μg of TM601 in one eye and vehicle in the fellow eye. After 2 days, ocular sections through choroidal NV from TM601-injected eyes showed TUNEL-positive cells that also stained with the vascular endothelial cell marker *G. simplicifolia* lectin (GSA) indicating apoptosis of cells participating in the choroidal NV (Fig. 2E–G). There were also TUNEL-positive cells in the overlying retina due to damage from the laser photocoagulation that had been used to rupture Bruch's membrane. At 9 days after rupture of Bruch's membrane, sections from eyes given periocular injections of 50 μg of TM601 on days 7 and 8 also showed TUNEL-positive, GSA-stained endothelial cells in choroidal NV (Fig. 2H–J). In contrast, ocular sections from eyes that had been injected with vehicle showed TUNEL-positive cells in overlying retina, but none within the choroidal NV (Fig. 2K–M). Therefore, intraocular or

periocular administration of TM601 caused apoptosis of endothelial cells localized to areas of NV.

TM601 suppresses ischemia-induced retinal NV

To determine the effect of TM601 on ischemia-induced retinal NV, we used the murine model of oxygen-induced ischemic retinopathy. At postnatal day (P) 12, mice with ischemic retinopathy were given an intraocular injection of 1 μl of vehicle in one eye and 50 μg of TM601 in the other eye. At P17, retinal NV was visualized on the surface of retinal flat mounts by in vivo immunostaining with anti-PECAM-1. Fluorescence microscopy images of entire retinas showed lesser amounts of NV on the surface of retinas from TM601-treated eyes than retinas from vehicle-treated eyes (Fig. 3A vs. B), with better visualization of individual tufts of NV seen at higher magnification (Fig. 3C,D). Image analysis confirmed that the mean area of NV per retina was significantly less in TM601-treated eyes compared to those treated with vehicle (E).

TM601 suppresses VEGF-induced retinal NV

Transgenic mice in which the *rhodopsin* promoter drives expression of VEGF in photoreceptors (rho/VEGF mice) develop extensive NV on the outer surface of the retina at P21 in the absence of ischemia (Okamoto et al., 1997; Tobe et al., 1998a). Between P7 and P21 rho/VEGF mice were given daily periocular injections of 3 μl of vehicle or vehicle containing 150 μg of TM601. Mice were perfused with fluorescein-labeled dextran at P21 and compared to retinal flat mounts from vehicle-treated mice (Fig. 4A–C) those from TM601-treated mice (Fig. 4D–F) showed less NV. Image analysis confirmed that TM601 significantly suppressed VEGF-induced retinal NV (Fig. 4G).

TM601 suppresses VEGF-induced vascular permeability

Mice were given an intraocular injection of 200 ng of VEGF, a mixture of 200 ng of VEGF and 50 μg of TM601, or vehicle and after 6 h, retinas were stained for serum albumin and PECAM-1 and examined by fluorescence microscopy. Retinas from eyes injected with VEGF alone showed large aggregates of albumin adjacent to retinal vessels (Fig. 5A–C). Retinas from eyes injected with a mixture of VEGF and TM601, showed substantially fewer clumps of albumin (Fig. 5D–F), and retinas from eyes injected with vehicle showed essentially no staining for albumin (Fig. 5G–I). Image analysis showed that TM601 significantly reduced VEGF-induced leakage of albumin into the retina (Fig. 5J).

TM601 selectively localizes to choroidal NV

Two days after intraocular injection of 50 μg of TM601 in eyes with established choroidal NV, staining of ocular sections for PECAM-1 showed the choroidal NV (Fig. 6A, arrows). Staining of the same sections with an antibody directed against TM601 showed a similar pattern of staining (Fig. 6B, arrows) and merged images showed co-localization of PECAM-1 and TM601 suggesting that TM601 was binding to vascular endothelial cells within the choroidal NV (Fig. 6C, arrows). When eyes with established choroidal NV were given periocular injections of TM601, a similar result was obtained (Fig. 6D–F, arrows) indicating that with two different routes of administration, TM601 homed to and selectively

bound to cells within choroidal NV. Eyes with choroidal NV that had intraocular injection of vehicle showed no staining for TM601 within PECAM-1-labeled choroidal NV (Fig. 6G–I, arrows).

We investigated the possibility that TM601 might be binding to annexin A2 on endothelial cells in new vessels, because TM601 complexes with annexin A2 on the surface of tumor cells and proliferating endothelial cells (Kesavan et al., 2010). Sections from eyes with choroidal NV that were injected with TM601 showed staining for annexin A2 in choroidal NV (Fig. 6J, arrows) that co-localized with staining for TM601 (Fig. 6K,L, arrows). Choroidal flat mounts from eyes with choroidal NV injected with TM601 showed staining for annexin A2 in the choroidal NV, but not surrounding normal choroidal vessels (Fig. 6M). There was co-localization of TM601 and annexin A2 within the choroidal NV (Fig. 6N,O). In eyes with ischemic retinopathy, there was selective staining for annexin A2 in buds of NV on the surface of the retina (Fig. 6P) and TM601 co-localized with the annexin A2 within the retinal NV (Fig. 6Q,R).

Other agents that bind to annexin A2 suppress retinal NV

We hypothesized that the endogenous ligands for annexin A2, plasminogen and tissue plasminogen activator (tPA) would stimulate retinal neovascularization, and that TM601 would block the stimulation. To test this hypothesis, we explored the effects of intraocular injections of plasminogen and tPA in mice with ischemic retinopathy. Contrary to our expectations, mice that had an intraocular injection of 0.5 μg of plasminogen (Fig. 7B) or 0.5 μg of tPA (Fig. 7C) at P12 had significantly less retinal NV than mice that were injected with vehicle (Fig. 7A,D).

Discussion

In this study, we have found that a small synthetic version of a peptide that was originally isolated from scorpion venom suppresses retinal and choroidal NV when injected into the vitreous cavity or when given by intravenous or periocular injections. Periocular injections of 10 μg of TM601 have a modest suppressive effect and a maximal effect is achieved with 50 μg which has a similar effect as injections of 250 or 1,000 μg of TM601. There was no suppression of choroidal NV in fellow eyes indicating that at doses up to 1,000 μg the major effect occurs from local penetration through the sclera and not absorption into the systemic circulation.

When TM601 was administered to eyes with established NV, it caused regression of the NV by inducing apoptosis in endothelial cells participating in the NV, but it had no effect on the endothelial cells in mature vessels. Immunohistochemical staining of areas of choroidal NV on choroidal flat mounts or in ocular sections of TM601-injected eyes with an antibody that specifically recognizes TM601 demonstrated that TM601 binds to endothelial cells participating in choroidal NV. When TM601 was injected into eyes with ischemic retinopathy, it localized to tufts of retinal NV and not normal retinal blood vessels. This suggests that TM601 binds to something that is not present or present in low amounts on normal retinal endothelial cells but is induced when those endothelial cells participate in neovascularization.

Pull down experiments have shown that TM601 binds to annexin A2 on the surface of tumor cells and proliferating vascular endothelial cells (Kesavan et al., 2010). There was no detectable immunohistochemical staining for annexin A2 on normal retinal and choroidal blood vessels, but there was prominent staining on vessels within retinal or choroidal NV. Consistent with TM601 binding selectively to annexin A2, eyes with NV that were injected with TM601 showed co-localization of annexin A2 and TM601. These data suggest that TM601 binds to annexin A2 that is induced on the surface of endothelial cells participating in retinal or choroidal NV.

Annexin A2 is a member of the annexin family of calcium-regulated phospholipid-binding proteins that has been implicated in the pathogenesis of ischemia-induced retinal NV (Ling et al., 2004). It is present in the cytosol of endothelial cells primarily as a monomer. Two annexin A2 molecules bind with two molecules of S100A10, a member of the S100 family of proteins, to form a heterotetramer, which increases the affinity of annexin A2 for phospholipids and calcium promoting membrane binding (Powell and Glenney, 1987). After the heterotetramer docks on the internal surface of the cell membrane, stress-induced phosphorylation of Tyr^{23} of the annexin A2 subunits by pp60-*c-Src* induces translocation to the cell surface (Deora et al., 2004). The increased immunostaining for annexin A2 in retinal and choroidal endothelial cells participating in NV compared to those in mature vessels is likely due to activation of pp60-*c-Src* causing enhanced translocation of the heterotetramer to the cell surface. TM601 binds to annexin A2 in tumor cells and proliferating endothelial cells (Kesavan et al., 2010) and thus it is reasonable to conclude that increased annexin A2/S100A10 heterotetramer on the surface of endothelial cells in new vessels is the basis for the ability of TM601 to home to the neovascularization regardless of its route of administration.

The function of annexin A2/S100A10 heterotetramer on the surface of endothelial cells is to promote normal fibrinolysis by acting as a co-receptor for plasminogen and tPA thereby greatly increasing the efficiency of plasminogen activation by tissue plasminogen activator (Cesarman et al., 1994; Hajjar et al., 1994). New vessels have very abnormal blood flow and may require a high level of fibrinolytic activity along their luminal surface to remain patent. Treatment of cultured vascular endothelial cells with TM601 inhibits VEGF and FGF2 stimulation of tissue plasminogen activator activity (Kesavan et al., 2010). Thus, binding of TM601 to annexin A2 may reduce fibrinolytic activity, promote thrombosis, and thereby induce apoptosis of the endothelial cells and regression of the NV. We hypothesized that increased binding of one of the endogenous ligands, plasminogen, or tPA in the setting of ischemic retinopathy would increase fibrinolytic activity and increase retinal NV and that TM601 would compete for annexin A2 binding and block plasminogen- or tPA-induced stimulation or retinal NV. Contrary to our expectations, intraocular injection of plasminogen or tPA in eyes with ischemic retinopathy reduced the amount of retinal NV. Perhaps the balance of endogenous plasminogen and tPA bound to annexin A2 in ischemic retina is critical and any disruption of that balance by injection of exogenous plasminogen or tPA reduces rather than increases local fibrinolytic activity. Perhaps anything that binds to annexin A2 will disrupt the delicate balance and suppress retinal NV. This hypothesis is supported by the demonstration that angiostatin, a proteolytic fragment of plasminogen that binds annexin A2, reduces fibrinolytic activity of cultured cells, and induces apoptosis of

endothelial cells and regression of NV (O'Reilly et al., 1994; Lucas et al., 1998; Tuszynski et al., 2002; Sharma et al., 2006). We also found that TM601 reduces VEGF-induced excessive vascular permeability. The mechanism of this anti-permeability effect is unclear, but there is evidence to suggest that angiostatin may also reduce excessive vascular leakage in the retina (Sima et al., 2004; Shyong et al., 2007).

Choroidal neovascularization due to AMD is the most prevalent cause of severe vision loss in elderly Americans. Ranibizumab, an Fab that blocks all isoforms of VEGF-A, causes significant improvement in vision in 34–40% of patients with choroidal NV due to AMD by reducing excessive leakage and suppressing growth of the NV (Brown et al., 2006; Rosenfeld et al., 2006). Ranibizumab does not cause regression of choroidal NV and continued intraocular injections are often required to maintain benefits. If TM601 causes regression of choroidal NV in humans as it does in mice, it may increase the duration of effect for treatments and add substantial benefit to anti-VEGF agents. Preliminary studies suggest that ranibizumab also provides benefit in diabetic macular edema, a prevalent cause of vision loss in working-age Americans (Nguyen et al., 2006b, 2009b). The anti-permeability effects of TM601 suggest that it may also be useful in that disease indication. Our data strongly support clinical trials investigating the effect of TM601 in neovascular AMD and diabetic macular edema.

Acknowledgments

The authors thank Jiangxia Wang and Carol B. Thompson of the core statistics module of NIH grant P30EY1765 for statistical consultation. This work was also supported by National Eye Institute (grant numbers EY12609 and EY009769) and TransMolecular, Inc.

Contract grant sponsor: National Eye Institute;

Contract grant number: EY12609, P30EY1765.

Contract grant sponsor: TransMolecular, Inc..

Literature Cited

Brown DM, Kaiser PK, Michels M, Soubrane G, Heier JS, Kim RY, Sy JP, Schneider S. Anchor Study Group. Ranibizumab versus verteporfin for neovascular age-related macular degeneration. N Engl J Med. 2006; 355:1432–1444. [PubMed: 17021319]

Campochiaro PA. Ocular versus extraocular neovascularization: Mirror images or vague resemblances. Invest Ophthalmol Vis Sci. 2006; 47:462–474. [PubMed: 16431938]

Cesarman GM, Guevara CA, Hajjar KA. An endothelial cell receptor for plasminogen and tissue plasminogen activator. II. Annexin II-mediated enhancement of t-PA-dependent plasminogen activation. J Biol Chem. 1994; 269:21198–21203. [PubMed: 8063741]

DeBin JA, Maggio JE, Strichartz GR. Purification and characterization of chlorotoxin, a chloride channel ligand from the venom of the scorpion. Am J Physiol. 1993; 264:C361–C369. [PubMed: 8383429]

Deora AB, Kreitzer G, Jacovina AT, Hajjar KA. An annexin 2 phosphorylation switch mediates p11-dependent translocation of annexin 2 to the cell surface. J Biol Chem. 2004; 279:43411–43418. [PubMed: 15302870]

Hajjar KA, Jacovina AT, Chacko J. An endothelial cell receptor for plasminogen and tissue plasminogen activator. I. Identity with annexin II. J Biol Chem. 1994; 269:21191–21197. [PubMed: 8063740]

Hockaday DC, Shen S, Fiveash J, Raubitschek A, Colcher D, Liu A, Alvarez V, Mamelak AN. Imaging glioma extent with 131I-TM-601. J Nucl Med. 2005; 46:580–586. [PubMed: 15809479]

Jacoby DB, Dyskin C, Yalcin M, Kesavan K, Dahlberg W, Ratliff J, Johnson EW, Mousa SA. Potent pleiotropic anti-angiogenic effects of TM601, a synthetic chlorotoxin peptide. Anticancer Res. 2010; 30:39–46. [PubMed: 20150615]

Kesavan K, Ratliff J, Johnson EW, Dahlberg W, Asara JM, Misra P, Frangioni JV, Jacoby DB. Annexin A2 is a molecular target for TM601, a peptide with tumor-targeting and anti-angiogenic effects. J Biol Chem. 2010; 285:4366–4374. [PubMed: 20018898]

Klein R, Klein BEK, Moss SE, Davis MD, DeMets DL. The Wisconsin Epidemiologic Study of Diabetic Retinopathy. II. Prevalence and risk of diabetic retinopathy when age at diagnosis is less than 30 years. Arch Ophthalmol. 1984; 102:520–526. [PubMed: 6367724]

Klein R, Klein BE, Linton KL. Prevalence of age-related maculopathy. The Beaver Dam Eye Study. Ophthalmology. 1992; 99:933–943. [PubMed: 1630784]

Lima e Silva R, Shen J, Hackett SF, Kachi S, Akiyama H, Kiuchi K, Yokoi K, Hatara C, McLauer T, Aslam S, Gong YY, Xiao WH, Khu NH, Thut C, Campochiaro P. The SDF-1/ CXCR4 ligand/ receptor pair is an important contributor to several types of ocular neovascularization. FASEB J. 2007; 21:3219–3230. [PubMed: 17522382]

Ling Q, Jacovina AT, Deora A, Febbraio M, Simantov R, Silverstien RL, Hempstead B, Mark WH, Hajjar KA. Annexin II regulates fibrin homeostasis and neoangiogenesis in vivo. J Clin Invest. 2004; 113:38–48. [PubMed: 14702107]

Lucas R, Holmgren L, Garcia I, Jimenez B, Mandriota SJ, Boriat F, Sim BK, Wu Z, Grau GE, Shing Y, Soff FA, Bouck N, Pepper MS. Multiple forms of angiostatin induce apoptosis in endothelial cells. Blood. 1998; 92:4730–4741. [PubMed: 9845539]

Mamelak AN, Rosenfeld S, Bucholz R, Raubitschek A, Nabors LB, Fiveash JB, Shen S, Khazaeli MB, Colcher D, Liu A, Osman M, Guthrie B, Schade-Bijur S, Hablitz DM, Alvarez VL, Gonda MA. Phase I single-dose of intracaitary-administered iodine-131-TM-601 in adults with recurrent high-grade glioma. J Clin Oncol. 2006; 24:3644–3650. [PubMed: 16877732]

Mori K, Ando A, Gehlbach P, Nesbitt D, Takahashi K, Goldsteen D, Penn M, Chen CT, Melia M, Phipps S, Moffat D, Brazzell K, Liau G, Dixon KH, Campochiaro PA. Inhibition of choroidal neovascularization by intravenous injection of adenoviral vectors expressing secretable endostatin. Am J Pathol. 2001; 159:313–320. [PubMed: 11438478]

Nguyen QD, Shah SM, Hafiz G, Quinlan E, Sung J, Chu K, Cedarbaum J, Campochiaro PA. CLEAR 0305 Study Group. A phase 1 trial of intravenously administered vascular endothelial growth factor (VEGF) trap for treatment in patients with choroidal neovascularization due to age-related macular degeneration. Ophthalmology. 2006a; 113:1522.e1–1522.e14. [PubMed: 16876249]

Nguyen QD, Tatlipinar S, Shah SM, Haller JA, Quinlan E, Sung J, Zimmer-Galler I, Do DV, Campochiaro PA. Vascular endothelial growth factor is a critical stimulus for diabetic macular edema. Am J Ophthalmol. 2006b; 142:961–969. [PubMed: 17046701]

Nguyen QD, Shah SM, Browning DJ, Hudson H, Sonkin P, Hariprasad SM, Kaiser P, Slakter JS, Haller J, Do DV, Mieler WF, Chu K, Yang K, Ingerman A, Vitti RL, Berliner AJ, Cedarbaum JM, Campochiaro PA. A phase I study of intravitreal vascular endothelial growth factor trap-eye in patients with neovascular age-related macular degeneration. Ophthalmology. 2009a; 116:2141–2148. [PubMed: 19700196]

Nguyen QD, Shah SM, Heier JS, Do DV, Lim J, Boyer D, Abraham P, Campochiaro PA. READ-2 Study Group. Primary end point (six months) results of the Ranibizumab for Edema of the mAcula in Diabetes (READ-2) Study. Ophthalmology. 2009b; 116:2175–2181. [PubMed: 19700194]

Okamoto N, Tobe T, Hackett SF, Ozaki H, Vinores MA, LaRochelle W, Zack DJ, Campochiaro PA. Transgenic mice with increased expression of vascular endothelial growth factor in the retina: A new model of intraretinal and subretinal neovascularization. Am J Pathol. 1997; 151:281–291. [PubMed: 9212753]

O'Reilly MS, Holmgren S, Shing Y, Chen C, Rosenthal RA, Moses M, Lane WS, Cao Y, Sage HE, Folkman J. Angiostatin: A novel angiogenesis inhibitor that mediates the suppression of metastases by a Lewis lung carcinoma. Cell. 1994; 79:315–328. [PubMed: 7525077]

Powell MA, Glenney JR. Regulation of calpactin I phospholipid binding by calpactin I light-chain binding and phosphorylation by p60v-src. Biochem J. 1987; 247:321–328. [PubMed: 2962567]

Rosenfeld PJ, Brown DM, Heier JS, Boyer DS, Kaiser PK, Chung CY, Kim RY. Marina Study Group. Ranibizumab for neovascular age-related macular degeneration. N Engl J Med. 2006; 355:1419–1431. [PubMed: 17021318]

Saishin Y, Saishin Y, Takahashi K, Lima Silva R, Hylton D, Rudge J, WSJ, Campochiaro PA. VEGF-$TRAP_{R1R2}$ suppresses choroidal neovascularization and VEGF-induced breakdown of the blood-retinal barrier. J Cell Physiol. 2003; 195:241–248. [PubMed: 12652651]

Sharma MC, Sharma M. The role of annexin II in angiogenesis and tumor progression: A potential therapeutic target. Curr Pharmacol Des. 2007; 13:3568–3575.

Sharma MR, Rothman V, Tuszynski GP, Sharma MC. Antibody-directed targeting of angiostatin's receptor annexin II inhibits Lewis lung carcinoma growth via blocking of plasminogen activation: Possible biochemical mechanism of angiostatin's action. Exp Mol Pathol. 2006; 81:136–145. [PubMed: 16643891]

Shen S, Khazaeli MB, Gillespie GY, Alvarez VL. Radiation dosimetry of 131I-chlorotoxin for targeted radiotherapy in glioma-bearing mice. J Neurooncol. 2005; 71:113–119. [PubMed: 15690125]

Shen J, Xie B, Dong A, Swaim M, Hackett SF, Campochiaro PA. In vivo immunostaining demonstrates macrophages associate with growing and regressing vessels. Invest Ophthalmol Vis Sci. 2007; 48:4335–4341. [PubMed: 17724225]

Shyong M-P, Lee F-L, Kuo P-C, Wu A-C, Cheng H-C, Chen S-L, Tung T-H, Tsao Y-P. Reduction of experimental diabetic vascular leakage by delivery of angiostatin with a recombinant adeno-associated virus vector. Mol Vis. 2007; 13:133–141. [PubMed: 17293777]

Sima J, Zhang SX, Shao C, Fant J, Ma J. The effect of angiostatin on vascular leakage and VEGF expression in rat retina. FEBS Lett. 2004; 564:19–23. [PubMed: 15094037]

Smith LEH, Wesolowski E, McLellan A, Kostyk SK, D'Amato R, Sullivan R, D'Amore PA. Oxygen-induced retinopathy in the mouse. Invest Ophthalmol Vis Sci. 1994; 35:101–111. [PubMed: 7507904]

Soroceanu L, Gillespie Y, Khazaeli MB, Sontheimer H. Use of chlorotoxin for targeting of primary brain tumors. Cancer Res. 1998; 58:4871–4879. [PubMed: 9809993]

Tobe T, Okamoto N, Vinores MA, Derevjanik NL, Vinores SA, Zack DJ, Campochiaro PA. Evolution of neovascularization in mice with overexpression of vascular endothelial growth factor in photoreceptors. Invest Ophthalmol Vis Sci. 1998a; 39:180–188. [PubMed: 9430560]

Tobe T, Ortega S, Luna JD, Ozaki H, Okamoto N, Derevjanik NL, Vinores SA, Basilico C, Campochiaro PA. Targeted disruption of the *FGF2* gene does not prevent choroidal neovascularization in a murine model. Am J Pathol. 1998b; 153:1641–1646. [PubMed: 9811357]

Tuszynski GP, Sharma MR, Rothman VL, Sharma MC. Angiostatin binds to tyrosine kinase substrate annexin II through the lysine-binding domain in endothelial cells. Microvasc Res. 2002; 64:448–462. [PubMed: 12453439]

Ullrich N, Bordey A, Gillespie GY, Sontheimer H. Expression of voltage-activated chloride currents in acute slices of human gliomas. Neuroscience. 1998; 83:1161–1173. [PubMed: 9502255]

Xie B, Shen J, Dong A, Swaim M, Hackett SF, Wyder L, Worpenberg S, Barbieri S, Campochiaro PA. An Adam15 amplification loop promotes vascular endothelial growth factor-induced ocular neovascularization. FASEB J. 2008; 22:2775–2783. [PubMed: 18381816]

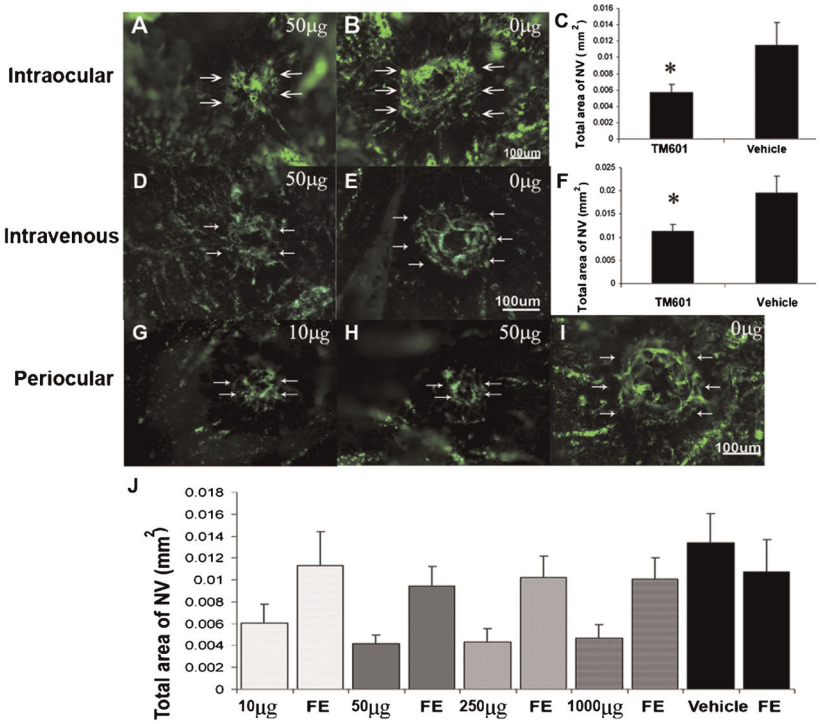

Fig. 1.

TM601 given by intraocular, intravenous, or periocular injections suppresses choroidal neovascularization (NV). Mice had laser photocoagulation-induced rupture of Bruch's membrane and then received an intraocular injection of 1 μl of vehicle or vehicle containing 50 μg of TM601. After 14 days, mice were perfused with fluorescein-labeled dextran and the area of choroidal NV at Bruch's membrane rupture sites was visualized by fluorescence microscopy of choroidal flat mounts and measured by image analysis. Other groups of mice had rupture of Bruch's membrane followed by tail vein injections of vehicle or 20 mg/kg of TM601 three times a week. The area of choroidal NV appeared smaller in eyes injected with TM601 (A) compared to those injected with vehicle (B). Statistical comparison using a mixed-effects model showed that the mean (±SEM) area of choroidal NV at Bruch's membrane rupture sites determined by image analysis with the investigator masked with respect to treatment group was less in eyes injected with TM601 compared to those injected with vehicle (C, $P = 0.013$). The area of choroidal NV was also significantly reduced in mice that received intravenous injections of TM601 compared to mice that received intravenous injections of vehicle (D–F, $P = 0.024$). Several different doses of TM601 were given by daily periocular injection. Representative images from eyes injected with 10 μg (G) or 50 μg (H) of TM601 show smaller areas of choroidal NV than a representative image from vehicle-injected eyes (I). Compared to eyes treated with vehicle, the mean (±SEM) area of choroidal NV at Bruch's membrane rupture sites was significantly less in eyes treated with daily periocular injections of each of the doses of TM601 (J, $P = 0.008$, 0.001, 0.001, and 0.002 for 10, 50, 250, and 1,000 μg, respectively). Eyes treated with 50 μg ($P = 0.007$), 250 μg ($P = 0.03$), or 1,000 μg ($P < 0.001$) ofTM601 had significantly smaller areas of choroidal NV than their corresponding untreated fellow eyes (FE). There was no significant difference in area of choroidal NV in eyes treated with 10 μg ofTM601 compared to corresponding fellow eyes ($P = 0.147$).

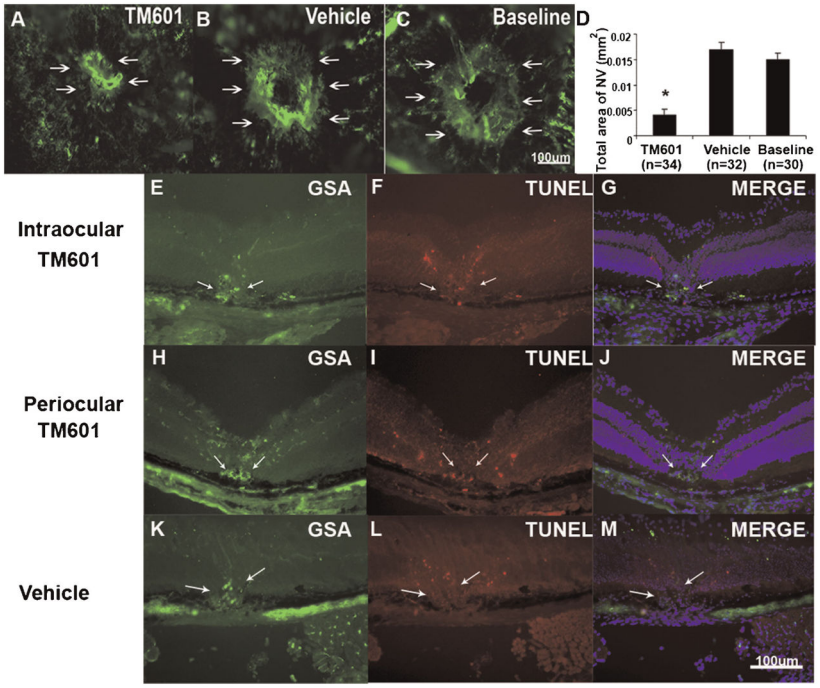

Fig. 2.

Intraocular injection of TM601 causes regression of established choroidal neovascularization (NV). Seven days after rupture of Bruch's membrane with laser photocoagulation, the baseline area of choroidal NV was measured in 10 mice. The 12 remaining mice were given an intraocular injection of 1 μl of vehicle in one eye and 1 μl of vehicle containing 50 μg of TM601 in the other eye. Seven days later, the area of choroidal NV at rupture sites appeared smaller in eyes injected with TM601 (A) compared to those in vehicle-injected eyes (B) or baseline eyes (C). Measurement of the area of choroidal NV by image analysis (D) showed that the mean area of choroidal NV in eyes injected with TM601 was significantly less than that in vehicle-injected or those in baseline eyes (P = 0.002 and 0.018 by a general estimating equations model). Mice had rupture of Bruch's membrane and after 1 week had an intraocular injection of 50 μg of TM601 in one eye (E–G) and vehicle in the fellow eye (K–M) or had daily periocular injections of 250 μg of TM601 (H–J). After 2 days, ocular sections through choroidal NV showed staining of the NV with *Griffonia simplicifolia* lectin (GSA), a vascular endothelial cell marker (E,H,K, arrows). Sections from eyes treated with TM601 showed TUNEL-positive, GSA-positive endothelial cells in the choroidal NV and also in the overlying retina from the laser treatment that induced the choroidal NV (F,G,I,J). Sections from vehicle-treated eyes showed TUNEL-positive cells in overlying retina, but none in the GSA-stained choroidal NV (L,M).

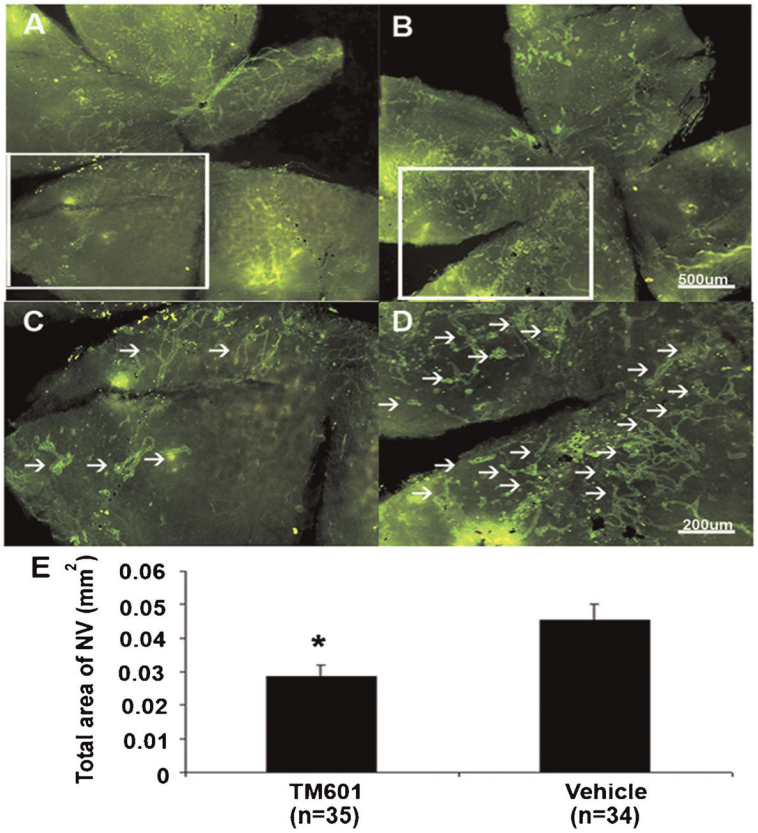

Fig. 3.

TM601 suppresses ischemia-induced retinal neovascularization. At postnatal day (P) 7, mice were placed in 75% oxygen and at P12 they were returned to room air and given an intraocular injection of 1 μl containing 50 μg of TM601 in one eye and vehicle in the other eye. At P17, *in vivo* immunostaining for PECAM-1 was done and retinal whole mounts were examined by fluorescence microscopy. Low power views of entire retinas from representative TM601-treated (A) and vehicle-treated (B) eyes show less neovascularization on the surface of the TM601-treated retina. Higher magnification of the boxed regions from (A) and (B) provide better resolution of individual tufts of neovascularization that are reduced in TM601-treated eyes (C) compared to vehicle-treated eyes (D). Image analysis with the investigator masked with respect to treatment group, showed that the mean (±SEM) area of NV on the surface of the retina was significantly less in TM601-treated eyes compared to those treated with vehicle (E, $P = 0.006$ by mixed-effects model).

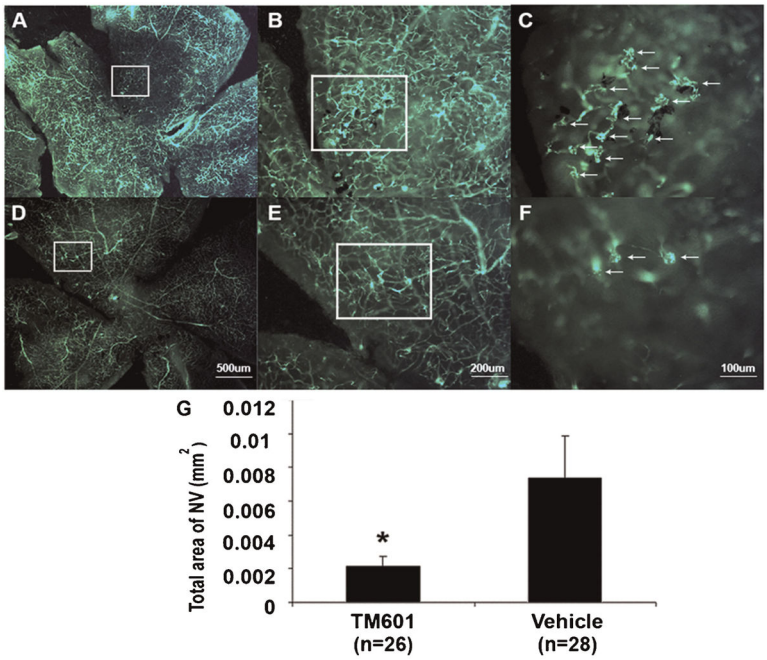

Fig. 4.

TM601 suppresses VEGF-induced subretinal neovascularization (NV) in *rhodopsin* promoter/*VEGF* (rho/VEGF) transgenic mice. Between P7 and P21 rho/VEGF mice were given daily periocular injections of 3 μl of vehicle or vehicle containing 150 μg of TM601. Mice were perfused with fluorescein-labeled dextran at P21. Retinal flat mounts from control, vehicle-treated eyes visualized with the photoreceptor side facing up showed extensive NV on the outer surface of the retina although it is difficult to see at the magnification that allows visualization of the entire retina because the normal retinal vessels are in the background (A). Higher magnification views (B,C) of the boxed region in (A) provides an arrow depth of field so that only the NV is in focus and the numerous tufts of NV that are partially surrounded by dark retinal pigmented epithelial cells are easily seen (C, arrows). Retinal flat mounts from TM601-injected eyes show much less NV (D); higher magnification of the boxed region in (D) shows few tufts of NV on the outer surface of the retina (E,F, arrows). Image analysis with the investigator masked with respect to treatment group showed that the mean (±SEM) area of NV per retina was significantly less fore yes treated with TM601 compared to controls (G). **P* = 0.017 for difference from control by mixed-effects model.

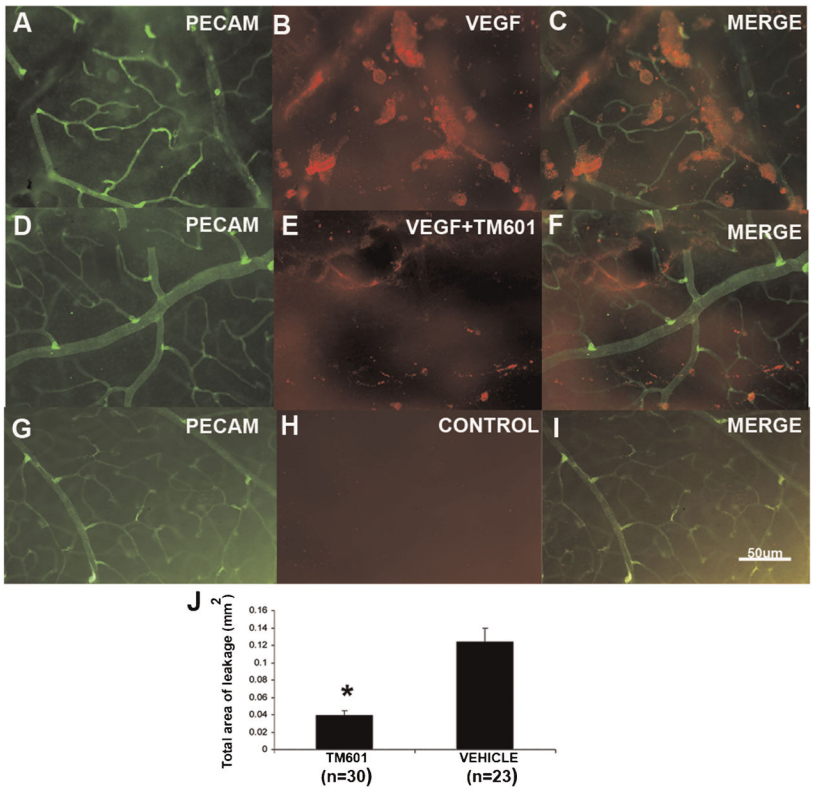

Fig. 5.

TM601 suppresses VEGF-induced retinal vascular permeability. Six hours after intraocular injections of VEGF, a mixture of VEGF and TM601, or vehicle, mice were euthanized and retinas were stained for serum albumin or PECAM-1. Retinas from eyes injected with vehicle only, showed no staining for albumin (G–I), when examined by fluorescence microscopy. Retinas from eyes injected with VEGF alone showed significantly more large aggregates of albumin adjacent to retinal vessels (A–C) comparing to retinas from eyes injected with a mixture of VEGF and TM601 (D–F). Measurement of the leakage area of albumin showed that TM601 significantly reduced VEGF-induced leakage of albumin into the retina ($P = 0.0001$ by ANOVA with Bonferroni/Dunn test).

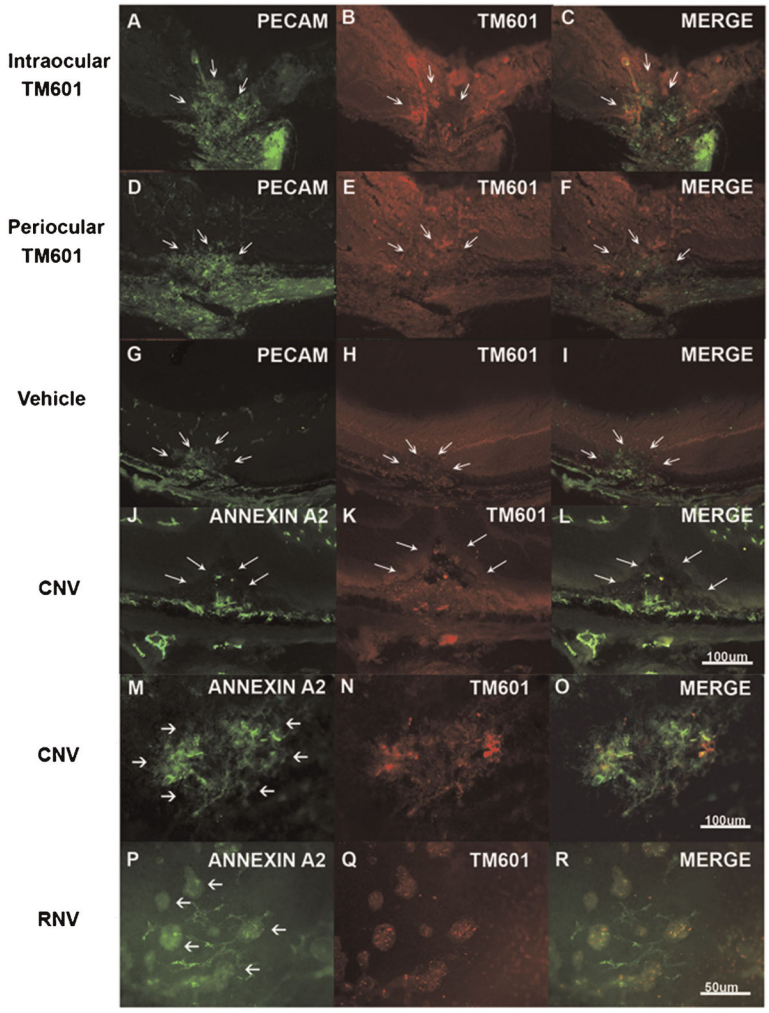

Fig. 6.

TM601 homes to retinal and choroidal neovascularization (NV) where it is co-localized with upregulated annexin A2. Mice had rupture of Bruch's membrane and after 1 week had an intraocular injection of 50 μg of TM601 in one eye (A–C) and vehicle in the fellow eye (G–I) or had daily periocular injections of 250 μg of TM601 (D–F). After 2 days, ocular sections through choroidal NV showed staining for PECAM-1 in the NV (A, arrows) and underlying choroidal vessels. Staining of the same section with an antibody that specifically recognizes TM601 showed strong immunofluorescence with a shape similar to the anti-PECAM-1 staining (B, arrows) and some mild background fluorescence throughout the retina. Merging of the images showed clear co-localization of TM601 and PECAM-1 (C, arrows). Eyes given periocular injections of TM601 also showed strong staining for TM601 in PECAM-1-labeled choroidal NV (D–F, arrows). Eyes given an intraocular injection of vehicle showed PECAM-1 staining of choroidal NV (G, arrows), but no staining for TM601 (H,I, arrows). Sections from eyes injected with TM601 showed staining for annexin A2 in choroidal NV (CNV,J, arrows) that co-localized with staining for TM601 (K,L, arrows). Achoroidal flat mount from an eye that had intraocular injection of TM601 7 days after rupture of Bruch's membrane showed intense staining of choroidal NV with anti-annexin A2 with no staining of surrounding choroidal vessels (M, arrows). There was also strong staining for TM601 thatco-localized with the staining for annexin A2 and with this technique there was minimal background staining (N,O). Similar experiments were done in mice with ischemic retinopathy to determine if annexin A2 is also upregulated in retinal NV and whether TM601 binds to retinal NV. At P17, mice with ischemic retinopathy were given and intraocular injection of 50 μg of TM601 and at P19, retinal flat mounts showed strong selective staining for annexin

A2 on tufts of retinal NV (RNV; P, arrows). Punctate staining for TM601 also occurred within the retinal NV (Q,R) indicating that annexin A2 is upregulated in retinal NV and TM601 binds in the areas of annexin A2 upregulation.

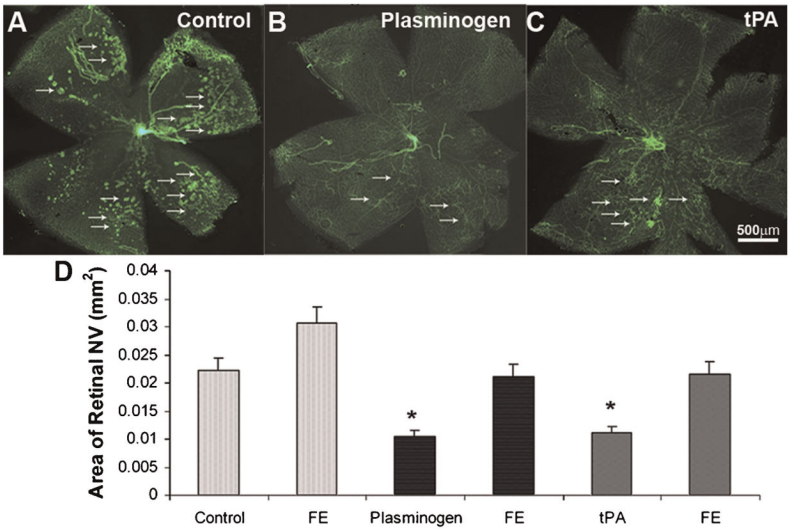

Fig. 7.

Effects of tPA or plasminogen in ischemia-induced retinal neovascularization (NV). C57BL/6 mice were placed in 75 ± 3% oxygen at P7. At P12 they were returned to room air and were given an intravitreous injection of 1 μl of vehicle or vehicle containing 0.5 μg of plasminogen or tissue plasminogen activator (tPA) in one eye. At P17, *in vivo* immunostaining for PECAM-1 was done and retinal flat mounts from eyes injected with plasminogen (B) or tPA (C) visualized with fluorescence microscopy showed less NV on the surface of the retina than eyes injected with vehicle (A). Quantification of the area of NV by image analysis is shown in (D). The bars show the mean (±SEM) area of NV and those for plasminogen (n =13) and tPA (n =8) were significantly less than respective control eyes injected with vehicle ($P < 0.05$ by unpaired *t*-test) or uninjected fellow eyes (FE).